

A Fractal Approach To Adsorption on Heterogeneous Solids Surfaces. 2. Thermodynamic Analysis of Experimental Adsorption Data

Wladyslaw Rudzinski,^{*,†} Shyi-Long Lee,[‡] Tomasz Panczyk,[†] and Ching-Cher Sanders Yan[‡]

Department of Theoretical Chemistry, Faculty of Chemistry, Maria Curie-Skłodowska University, Place Marii Curie-Skłodowskiej 3, Lublin, 20-031 Poland, and Department of Chemistry, National Chung-Cheng University, 160, San Hsing, Ming-Hsiung, Chia-yi, 621 Taiwan, Republic of China

Received: April 2, 2001; In Final Form: July 3, 2001

The isotherm equations developed in part I of this publication have been further generalized to account for the effects of multilayer adsorption. This was done employing the fractal BET isotherm developed by Fripiat et al. Their BET equation takes into account the geometric effects of fractality on the formation of second and subsequent layers, but ignores the energetic effects of fractality on adsorption in the first layer, closest to the surface. To correct this, their expression was integrated with the generalized adsorption energy distribution developed in part I (Rudzinski, W.; Lee, S.-L.; Panczyk, T.; Yan, C.-C. *S. J. Phys. Chem. B* 2001, 105, 10847). Using the generalized fractal BET equation obtained in this way, we are able to correlate the experimental data from the lowest pressures investigated up to the surface loadings approaching coverage by two layers. Two adsorption systems have been subjected to this analysis. One was nitrogen adsorbed on a commercially available silica, and the second nitrogen adsorbed by a commercially available activated carbon. As a result of these fittings, there have been obtained the parameters characterizing both the geometric and energetic heterogeneities of these two gas/solid systems.

Results and Discussion

1. Adsorption at Submonolayer Coverages. Let us consider adsorption at submonolayer surface coverages, where θ_t is given by eq 38 in the first part of this publication. The value of r_0 depends on the choice of ϵ_0 ; so from now on, we will choose ϵ_0 in such a way that $r_0 = 1$. Then, at low surface coverages, eq I.38 (eq 38 of part I)²⁸ reduces to eq I.12.²⁸ Depending on the values of adsorbate pressure, either the Freundlich term $-\alpha(\epsilon_c - \epsilon_0)$ or the DR term $-\beta(\epsilon_c - \epsilon_0)^2$ will dominate the behavior of the adsorption isotherm.

The appearance of the pressure regions, where either the Freundlich or the DR behavior will dominate, depends on the nature of an adsorption system characterized by the values of p_0 , $(\partial F/\partial \epsilon)_{\epsilon_0}$, and those of $(\partial^2 F/\partial \epsilon^2)_{\epsilon_0}$. However, it is assumed that, in general, the behavior of θ_t at low pressures (surface coverages) will be a hybrid between the Freundlich and the DR behavior, i.e., θ_t could be correlated by the Dubinin–Astakhov equation.^{1,2}

$$\ln \theta_t = -\gamma(\epsilon_c - \epsilon_0)^r = -(kT\gamma)^r \left[\ln \frac{p_0}{p} \right]^r, \quad 1 < r < 2 \quad (1)$$

This is frequently observed in many adsorption systems. There is a large body of the published papers reporting on the wide use of the DA isotherm.^{1,2}

It has been a common practice to put $p_0 = p_s$, in both the DR and the DA isotherm equations. However, it is to be noted, that p_0 cannot, in general, be identified with the value of the

saturation pressure p_s at the investigated temperature. The assumption that $p_0 = p_s$ comes from the classical viewpoint of Polanyi that adsorption is a compression of adsorbate molecules by gas–solid forces to a liquidlike state in pores. In the case of heterogeneous surfaces, the adsorption takes place in pores having limited dimensions.

Computer simulations of adsorption in pores carried out so frequently show, that the state of the adsorbate in pores may be distinctly different from that in a bulk liquid.³ In the picture of the localized adsorption in pores, the meaning of p_0 in eq I.14a²⁸ is determined by the statistical development of the Langmuir isotherm,

$$K = q_0^s \exp\left(\frac{\mu_0^s}{kT}\right) \quad (2)$$

where q_0^s is the product of the three vibrational partition functions, and of the other ones (vibrational or rotational, electronic, spin, etc.), whereas μ_0^s is the standard chemical potential of gas adsorbate, defined also in appropriate statistical-thermodynamic considerations. Identification of p_0 with p_s which has not been sufficiently realized in the hitherto analyses of experimental adsorption isotherms may lead to serious confusion and misleading results, as shown below.

Let us consider for that purpose the region of low surface coverages, where eq I.38²⁸ reduces to eq I.12,²⁸ which can be rewritten to the following form,

$$\begin{aligned} \ln N_t &= \ln M - \alpha(\epsilon_c - \epsilon_0) - \beta(\epsilon_c - \epsilon_0)^2 + \dots \\ &= \ln M + A_0 - A_1 kT \left[\ln \frac{p}{p_s} \right] - A_2 (kT)^2 \left[\ln \frac{p}{p_s} \right]^2 \end{aligned} \quad (3)$$

* To whom correspondence should be addressed.

[†] Department of Theoretical Chemistry.

[‡] Department of Chemistry.

where ϵ_c is given in eq I.20a,²⁸ and where

$$A_0 = (\epsilon_0 - \epsilon_k)[\alpha - \beta(\epsilon_0 - \epsilon_k)] \quad (3a)$$

$$A_1 = 2\beta(\epsilon_0 - \epsilon_k) - \alpha \quad (3b)$$

$$A_2 = \beta \quad (3c)$$

$$\epsilon_k = -kT \ln Kp_s \quad (3d)$$

Equation 43 shows that even with an incorrect choice of p_0 (this time $p_0 = p_s$), one should observe a fairly linear dependence of $\ln N_t$ on $[\ln(p_s/p)]^2$ at sufficiently low coverages, and that the tangent of that linear section could tend to the value of β . However, when $\ln N_t$ is plotted against $\ln(p_s/p)$, the quadratic dependence of $\ln N_t$ on $\ln(p_s/p)$ should be observed.

For the purpose of illustration, we have taken the data discussed in two papers by Dr. Ehrburger-Dolle,^{4,5} which we had at our disposal owing to the courtesy of the author.

These are isotherms of nitrogen adsorption on various carbonaceous, and silica materials. The isotherms were measured from pressures like 10^{-6} (p/p_s), up to (p/p_s) close to unity. Ehrburger-Dolle also has presented a discussion based on the existing adsorption theories, as well as on using some semiempirical power-law expressions, proposed by the author. This time, we use these data to verify the concept of the surface heterogeneity launched in this paper.

For the purpose of illustration, we have chosen two adsorption systems with the largest number of the reported experimental points. One of them was nitrogen adsorbed by Aerosil 200, a fume silica produced by Degusa, and obtained by phyrohydrolysis of SiCl_4 . It was a hydrophilic amorphous silica, whose area estimated by the BET method was $217 \text{ m}^2/\text{g}$. (The corresponding monolayer capacity M was 2.23 mmol/g).

The other adsorption system was nitrogen adsorbed by carbon black TN330, produced by Tokai Carbon. Its BET surface area was estimated to be $69 \text{ m}^2/\text{g}$, from the corresponding monolayer capacity $M = 0.71 \text{ mmol/g}$.

Figures 1 and 2 show $\ln N_t$ plotted both as the function of $kT [\ln(p_s/p)]$, and of $(kT)^2 [\ln(p_s/p)]^2$. The rapid change in the tangent of the plots $\ln N_t$ vs $kT [\ln(p_s/p)]$ close to $p_s/p = 1$ is due to overwhelming multilayer adsorption, but this tangent does not tend to a constant value at still lower and lower pressures. Instead, the plots $\ln N_t$ vs $kT [\ln(p_s/p)]$ have an inflection point at some small pressures indicating that $\ln N_t$ decreases there with the power of $kT [\ln(p_s/p)]$ higher than one. The plots $\ln N_t$ vs $(kT)^2 [\ln(p_s/p)]^2$ show that this is the quadratic term on the rhs of eq 3 which becomes dominant at the lowest adsorbate pressures, just as predicted by our generalized adsorption energy distribution. At these lowest pressures the plot $\ln N_t$ vs $(kT)^2 [\ln(p_s/p)]^2$ becomes fairly linear.

Following eq 3, the experimental $\ln N_t$ points should be described by a quadratic function of $kT \ln(p_s/p)$. We made such approximation for a certain number of experimental points corresponding to the lowest investigated pressures up to the inflection point on the isotherm. The solid lines in Figures 1 and 2 show that approximation. The black circles show the $\ln N_t$ function from which the quadratic term $-(kT)^2 [\ln(p_s/p)]^2$ was subtracted. Such behavior of $\ln N_t$ plotted vs $-kT \ln(p_s/p)$ is never found in experiment which illustrates the important role of the quadratic term at low surface coverages.

The solid line in Figure 2 is a decreasing function at high adsorbate pressures. Thus, despite an apparently good quadratic approximation, this solid line cannot be interpreted in terms of eq 3, which is a fully rigorous expression when the surface is

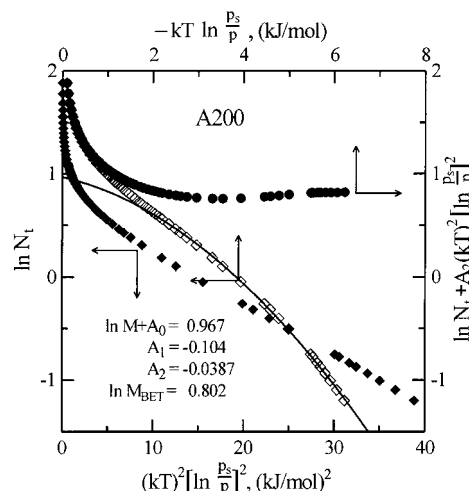


Figure 1. Application of eq 3 to analyze the experimental data for nitrogen adsorbed by the A200 silica at 77 K. The experimental $\ln N_t$ points are plotted both as a function of $-kT \ln(p_s/p)$ (\diamond) and as a function of $(kT)^2 [\ln(p_s/p)]^2$ (\blacklozenge). The solid line (—) is the approximation by the quadratic function of $[\ln(p_s/p)]$ defined on the right-hand side of eq 3, of the first 15 experimental $\ln N_t$ points corresponding to the lowest surface coverages, up to the inflection point observed on the experimental $N_t(\ln(p_s/p))$ curve (\diamond). The obtained best-fit parameters, A_0 , A_1 , and A_2 are displayed. The solid circles (\bullet) display the behavior of the $\ln N_t$ function from which the quadratic term $-A_2(kT)^2 [\ln(p_s/p)]^2$ was subtracted to demonstrate its importance.

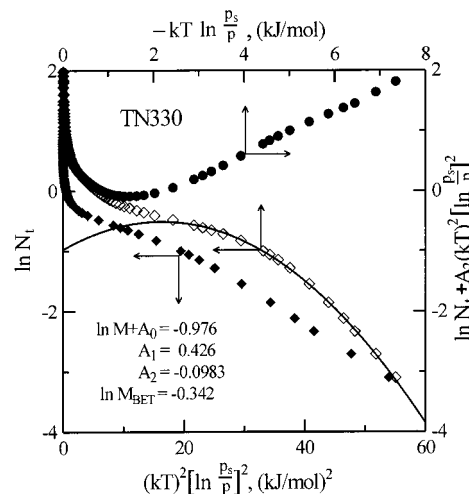


Figure 2. Application of eq 3 to analyze the experimental data for nitrogen adsorbed by the activated carbon TN330 at 77 K. Other details are the same as in Figure 1.

fully fractal. (The function $\chi(\epsilon)$ is then given by eq I.37²⁸). Thus, according to eq I.38,²⁸ the quadratic function should be considered as equal to $\ln[\theta_v/(1 - \theta_v)]$

$$\ln \frac{N_t/M}{1 - N_t/M} = A_0 - A_1 kT \left[\ln \frac{p_s}{p} \right] - A_2 (kT)^2 \left[\ln \frac{p_s}{p} \right]^2 \quad (4)$$

Figure 3 shows the approximation of the experimental function $\ln[N_t/M/(1 - N_t/M)]$ by this quadratic function.

To carry out this approximation, we had to assume a certain value of M . One can see in Figure 3, that while taking the BET value of $M = 0.71 \text{ mmol/g}$, the quadratic function is still a decreasing function of p at higher p/p_s values. However, in the region of submonolayer coverages where effects of multilayer adsorption are negligible, $\ln[\theta_v/(1 - \theta_v)]$ should be an increasing function of pressure according to its physical meaning. The first

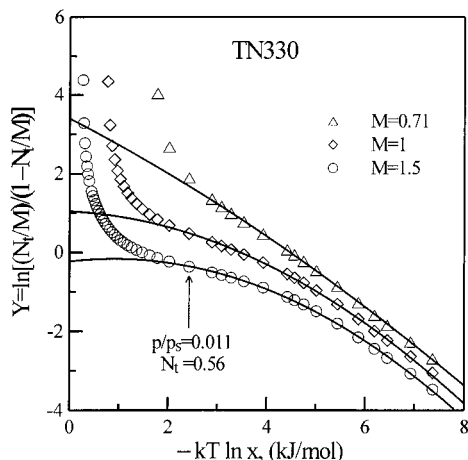


Figure 3. Application of eq 4 to analyze the experimental data for nitrogen adsorption by TN330. The solid lines (—) represent the best fit, by the quadratic function defined on the right-hand side of eq 4, of the first 15 experimental points, up to the inflection point.

nondecreasing quadratic function is obtained by assuming that $M \approx 1$ mmol/g.

That result confirms what has already been known for a long time. Namely, that, in the case of heterogeneous surfaces, using the standard BET method leads to underestimation of the value of M . This has been demonstrated by Cortes and Araya.⁶ They took a BET isotherm as the local isotherm $\theta(\epsilon, p, T)$ (kernel) under the integral in eq I.1,²⁸ and averaged it with a Gaussian adsorption energy distribution $\chi(\epsilon)$. In that way they generated an actual adsorption isotherm for such an energetically heterogeneous surface. Then they analyzed it using the standard BET method. The recovered values of M were smaller than the known true value of M . The larger the assumed variance of $\chi(\epsilon)$, the stronger the underestimation of M was observed.

Looking at Figure 3, one can see that, in the case of the investigated activated carbon TN330, one has to assume that $M \geq 1$ mmol/g. That means using the standard BET method underestimates the recovered value of M by more than 30%. However, Figure 3 shows that even choice of as high as 1.5 mmol/g value of M makes it possible to fit by the quadratic function only the same number of the first 15 experimental points $\ln[N_t/M/(1 - N_t/M)]$ corresponding to the lowest pressures, which we could fit in Figure 2. It is obvious that, to achieve such a quadratic fit for a larger number of experimental points, we must take into account the effects of multilayer adsorption.

2. Multilayer Adsorption on Heterogeneous Surfaces. It is well-known that, in the case of energetically heterogeneous surfaces, adsorption processes have much more mixed monolayer/multilayer character than in the case of adsorption on homogeneous solid surfaces. On highly energetic areas (sites) of surface, multilayer formation begins at relatively smaller pressures, long before the monolayer coverage is fairly completed on less energetic areas (sites) of the surface. It is also well-known, that theoretical description of “multilayer” adsorption on heterogeneous surfaces is one of the most challenging problems of adsorption science. Most commonly, the attempts to construct such a description went toward improving the BET model for that purpose.

The main criticism of the BET model concerns its applicability in the region of high coverages where the statistical number of adlayers is much higher than one. The slab (FHH) models are generally applied there.^{1,7–13} At the same time BET model is believed to be a fairly realistic picture of adsorbed phase at

surface coverages not far from the statistical monolayer coverage. Therefore, it comes as no surprise that various attempts were made to further improve the BET model by taking the “energetic” and the “geometric” heterogeneities into account; and again, considering the energetic and geometric heterogeneities went along two separate paths. A certain exception was the work by the group in Lublin, Poland, where the BET equation developed for a finite number of layers was further generalized by taking into account the energetic surface heterogeneity.¹⁴ These papers appeared at the beginning of the seventies of the 20th century, when the fractal approach was not published yet. Therefore, they could not take into account the restrictions imposed on multilayer formation by the fractal geometry of the actual solid surfaces.

Some 10 years later there were published two theoretical papers, one by Cole et al.¹⁵ and the other one by Fripiat et al.¹⁶ where these geometric restrictions were already considered in terms of the fractal approach. However the BET constant was assumed to be the same for every surface site, i.e., these works ignored the effects of surface energetic heterogeneity.

However, the theoretical method applied by Fripiat et al.¹⁶ is very attractive, because it leads to a simple result which can still be improved, by allowing the BET constant C to vary. As a starting point for our consideration, we write the accurate form of the BET equation, obtained by the well-known simple statistical development,¹⁷

$$\frac{N}{M} = \frac{1}{1 - q \exp\left(\frac{\mu}{kT}\right)} \frac{q_1 \exp\left(\frac{\mu}{kT}\right)}{1 - q \exp\left(\frac{\mu}{kT}\right) + q_1 \exp\left(\frac{\mu}{kT}\right)} \quad (5)$$

where q_1 is the molecular partition function of the molecules adsorbed in the first layer, whereas q is for the molecules adsorbed in the second and higher layers. The BET constant C is the ratio (q_1/q) , and μ is the chemical potential, usually expressed as the potential of an ideal gas in the bulk equilibrium gas phase.

$$\mu = \mu_0 + kT \ln p \quad (5a)$$

The term $q \exp(\mu/kT)$ can be written as (p/p_s) , only if the state of the molecules adsorbed in the second and higher layers is identical with the state of the bulk liquid at the same temperature. Such an assumption is commonly made, but we are not forced to accept it. Let us denote by p'_0 the value,

$$p'_0 = \frac{1}{q} \exp\left(-\frac{\mu'_0}{kT}\right) = \frac{1}{K} \quad (6)$$

The BET eq 5 takes then the following form

$$\frac{N}{M} = \frac{1}{1 - x} \frac{\frac{x}{1 - x} \exp\left(\frac{\epsilon}{kT}\right)}{1 + \frac{x}{1 - x} \exp\left(\frac{\epsilon}{kT}\right)} \quad (7)$$

where

$$x = \frac{p}{p'_0} \quad (7a)$$

When one assumes that only a limited number n of adlayers can be formed, the BET equation takes the following form:

$$\theta = \phi(x) \theta_m(x, \epsilon) \quad (8)$$

where $\theta_m(x, \epsilon)$ describes approximately the surface coverage in the first adsorbed layer, whereas $\phi(x)$ is mainly related to the multilayer formation.

$$\theta_m = \frac{c(\epsilon)X}{1 + c(\epsilon)X} \quad (9)$$

where

$$c = \exp\left(\frac{\epsilon}{kT}\right), \text{ and } X = \sum_{i=1}^n x^i \quad (9a)$$

Then,

$$\phi(x) = \frac{\sum_{i=1}^n ix^i}{X} \quad (10)$$

Therefore, while considering adsorption on energetically heterogeneous solid surfaces, Rudzinski et al.¹ wrote θ_t in the following form:

$$\theta_t = \int_0^\infty \phi \theta_m \chi \, d\epsilon = \phi \int_0^\infty \frac{c(\epsilon)X}{1 + c(\epsilon)X} \chi(\epsilon) \, d\epsilon \quad (11)$$

While assuming that the surface energetic heterogeneity is caused by the fractal nature of the real solid surfaces, the averaging eq 11 takes only into account the “energetic” effect of the surface fractality on the molecules adsorbed in the first layer closest to the solid surface, but ignores the geometric restrictions imposed by the fractal surface geometry on the formation of higher layers.

3. Generalizations of the BET Model to Describe both energetic and Geometric Fractality Effects. On the contrary, the paper by Fripiat et al.¹⁶ ignored the energetic effect of the fractal geometry on the first adsorbed layer, and focused on the modification of the function $\phi(x)$ describing multilayer formation, caused by the fractal nature of solid surfaces. Using a smart combination of computer simulations and analytical approaches, Fripiat et al. have arrived at the following form of the function $\phi(x)$, describing multilayer formation on the fractal surfaces.

$$\phi(x) = \frac{1}{X} \sum_{i=1}^n i^{2-D} \sum_{j=i}^n x^j \quad (12)$$

In the limit $D \rightarrow 2$, eq 12 reduces to the “classical” BET function (eq 10) for the finite number of the layers n .

It seems natural to combine the earlier treatment by Rudzinski et al.¹ with the treatment by Fripiat et al.¹⁶ to take into account both these effects, i.e., the “energetic” effects due to surface fractal nature on the adsorption in the first layer, and the geometric fractality effects on the multilayer formation. This can be done by replacing in eq 11 the “classical” BET function $\phi(x)$, by the “fractal” BET function $\phi(x)$, defined in eq 12.

As in the case of monolayer adsorption, the integration in eq 11 will be done by applying the condensation approximation approach, in which ϵ_c is found from the relation,

$$\left(\frac{\partial^2 \theta_m}{\partial \epsilon^2}\right)_\epsilon = \epsilon_c = 0 \quad (13)$$

leading to the following expression for ϵ_c

$$\epsilon_c = -kT \ln X \quad (14)$$

Therefore, the isotherm equation taking into account multilayer adsorption reads,

$$\begin{aligned} \frac{N_t}{M\phi} &= \left[1 + \exp\left\{(3-D)F'_0(\epsilon_c - \epsilon_0) + \frac{3-D}{2}F''_0(\epsilon_c - \epsilon_0)^2 + \dots\right\} \right]^{-1} = \\ &= \frac{\exp\{-\alpha(\epsilon_c - \epsilon_0) - \beta(\epsilon_c - \epsilon_0)^2 + \dots\}}{1 + \exp\{-\alpha(\epsilon_c - \epsilon_0) - \beta(\epsilon_c - \epsilon_0)^2 + \dots\}} \end{aligned} \quad (15)$$

where ϵ_c is now given in eq 14. This simple equation, developed by accepting the modified fractal model of the real solid surfaces, should describe the behavior of the real adsorption systems from very low pressures, up to those above the statistical monolayer coverage

Cole et al.¹⁵ proposed another modification of the “classical” BET equation for the case of the fractal surfaces. They assumed that fractal geometry manifests itself by changing monolayer capacity for the molecules adsorbed in the first layer closest to surface, and by the limitations imposed by r value on the maximum number of layers n which can be formed. At the same time, they ignored the fractal geometrical effects on the maximum number of molecules which can be adsorbed in the second and higher layers. Therefore, they assumed that the classical BET equation, developed for the finite number of layers n , should be averaged with respect to n , with the fractal pore sizes distribution. For that purpose, they write the BET equation in the following form:

$$\theta = \frac{cx}{1-x} \frac{1 - (n+1)x^n + nx^{n+1}}{1 + (c-1)x - cx^{n+1}} \quad (16)$$

Further, they assume that $r = nr_a$, where r_a is the radius of the adsorbed molecules. Then, the fractal BET equation should be written as follows:

$$N_t = M_f \frac{cx}{1-x} \frac{g(x)}{g(0)} \quad (17)$$

where

$$g(x) = \int_1^{r_m/r_a} \frac{1 - (n+1)x^n + nx^{n+1}}{1 + (c-1)x - cx^{n+1}} n^{1-D} \, dn \quad (18)$$

and M_f is the monolayer (surface area) capacity calculated by taking the fractal nature of the solid surface into consideration.

Equation 18 cannot be analytically integrated to express the new fractal BET isotherm in a simple compact form. We emphasize that both Fripiat et al.¹⁶ and Cole et al.¹⁵ did not take into account the variation in $c(\epsilon)$ with the varying pore size. This reflects the general trend in the hitherto studies of adsorption on fractal surfaces to consider only the related geometric restrictions. The existence of the accompanying energetic heterogeneity has not been realized until now, with very few exceptions. One of them is the above-discussed paper by Cole et al.¹⁵ where they discussed the effect of surface fractality on Henry's region of adsorption.

Thus, the difference between the approach by Fripiat et al., and that by Cole et al., is that the former authors assumed the

changing monolayer capacity in the adsorbed layers as the main effect of the surface fractality, whereas Pfeifer et al. assumed that this is the geometrical fractal restriction imposed on the maximum number of layers which can be formed. Of course, both these effects do exist, and the only question is which one is more important in a certain physical regime.

We believe that at the surface coverages not far from the statistical monolayer, the effect related to the changes in monolayer capacity in the first and the higher adsorbed layers should be more essential. But then, one has to make a decision which value of n should be accepted in the generalized fractal BET eq 15. We will treat the value of n as a parameter leading to reasonable fit of experimental data in the region of multilayer adsorption.

For that purpose we write eq 15 in the following form,

$$\ln \frac{N_t/(M\phi)}{1 - N_t/(M\phi)} = A_0 - A_1 kT \ln X - A_2 (kT)^2 [\ln X]^2 \quad (19)$$

where now

$$A_0 = \epsilon_0(\alpha - \beta\epsilon_0) \quad (19a)$$

$$A_1 = 2\beta\epsilon_0 - \alpha \quad (19b)$$

$$A_2 = \beta \quad (19c)$$

While choosing M properly, p'_0 , n , and D , the quadratic function of $\ln X$ on the right-hand side of eq 19 should fit a much greater number of the experimental points of $\ln[(N_t/M\phi)/(1 - N_t/M\phi)]$ than the first 15 points in Figure 2.

4. Application of the Generalized Fractal BET Equations.

A variety of methods have been proposed to determine the fractal dimension D . The most interesting ones are, of course, methods which utilize one adsorption isotherm as a source of experimental information. This is because it is the most easily and commonly measured observable. Such methods are in focus of our interest here, because only experimental adsorption isotherms are subjected to our theoretical analysis.

Following the theoretical works by Pfeifer,⁷ the fractal dimension D could be deduced from the part of the experimental adsorption isotherm corresponding to very high surface coverages where the adsorbed phase can be considered as a thick "slab". For that region of surface coverages Pfeifer, Kenntner, and Cole⁷ have developed the "fractal FHH" isotherm, suggesting that $\ln N_t$ should be a linear function of $\ln [kT \ln(p_0/p)]$, with a tangent equal to $(D - 3)$. Later on Avnir and Jaroniec⁹ and Yin¹³ proposed still other derivations of that "fractal FHH" isotherm.

Figure 4 shows our attempts to recover the D value for nitrogen adsorbed by the A200 silica and by the TN330 activated carbon, from the corresponding plots $\ln N_t$ vs $\ln[kT \ln(p_0/p)]$.

Recovering the fractal dimension D from the plots shown in Figure 4 is related to a number of uncertainties. On one hand, the adsorbed film must be thick enough for the "slab" approach to be applied. On the other hand, the growing thickness of the adsorbed film causes the "defractalization" of the slab discussed by Cheng, Cole, and Pfeifer.¹⁰ In fact, looking at Figure 4 we may see that the estimated fractal dimension D decreases with the growing adsorbed amount in the region of the highest surface coverages. In the case of the activated carbon TN330, the value of D takes then unrealistically low values.

Another uncertainty is raised by the alternative developments of the fractal FHH isotherm, published by Avnir and Jaroniec⁹

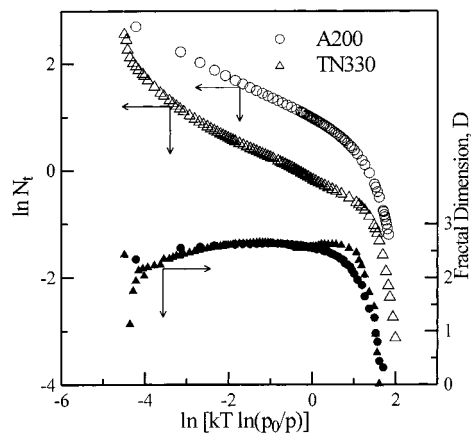


Figure 4. Application of the nonclassical "fractal FHH" isotherm to recover the value of the fractal dimension D . The open circles (\circ) are the values of $\ln N_t$ for the nitrogen adsorption by the A200 silica, whereas the open triangles (\triangle) are for nitrogen adsorption by the activated carbon TN330. The solid circles (\bullet) and the solid triangles (\blacktriangle) are the recovered (local) values of D for the A200 and TN330 adsorbents, respectively.

and by Yin.¹³ These derivations are based on somewhat different assumptions. Terzyk et al.^{18–22} have proposed a method in which the fractal dimension D is only one of the four best-fit parameters which might be found by fitting experimental isotherm by their fractal equation. However, like in the case of the Avnir–Jaroniec method, strong tendencies to multilayer adsorption may create certain problems in their application. Meanwhile the adsorption isotherms studied by us clearly show important contribution from multilayer adsorption. So, for the systems studied here by us, we have developed our own fractal isotherm equation taking explicitly into account effects due to multilayer adsorption.

Thus, we decided to check which values of D lead to the best reasonable fits of experimental adsorption data by our new fractal isotherm equation.

First we took the experimental data for nitrogen adsorption by the activated carbon TN330 into consideration. Our strategy of fitting these experimental data was following.

We took $M = 1$ mmol/g as the value of M , and assumed a certain pair of values, n and D . For these values of n and D , we calculated the discrete values of the function Y ,

$$Y = \frac{N_t/(M\phi)}{1 - N_t/(M\phi)} \quad (20)$$

from the experimental points $N_t(p/p_0)$. Next, we fitted the values of Y by the quadratic function defined on the rhs of eq 19. The philosophy behind that fit was following.

Provided that n and D are correctly chosen, the quadratic function should fit not only the first 15 points as in Figure 2, but also a certain number of points corresponding to much higher pressures and coverages where the fractal BET model still represents the mechanism of adsorption. After having performed hundreds of such numerical exercises, we found, that the pair of values $n = 4$ and $D = 2$ leads to the best agreement between theory and experiment. The corresponding best fit is shown in Figure 5.

Our finding is in excellent agreement with the estimation of typical D values of partially graphitized carbon blacks, made by using other methods, and reported by Avnir et al.²³

We can see in Figure 5 that the generalized BET fractal isotherm (eq 19) makes it possible to fit experimental data in

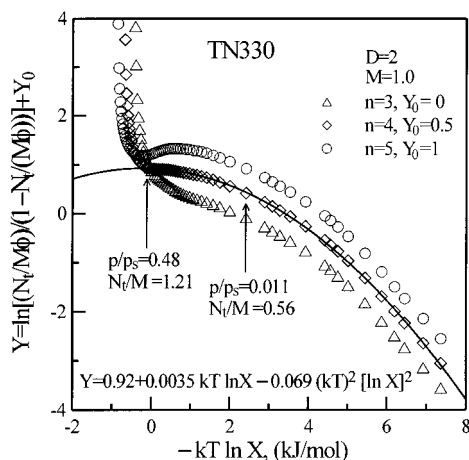


Figure 5. Application of eq 19 to correlate the experimental data for nitrogen adsorbed by the TN330 activated carbon. The solid line (—) is the approximation by the quadratic function defined in eq 19 of all the experimental points, up to the inflection point on the experimental $Y(p/p_s)$ curve. The related coefficients A_0 , A_1 , and A_2 are displayed. One arrow indicates the value $p/p_s = 0.48$ and $N_t/M = 1.21$ corresponding to this inflection point. The other arrow indicates $p/p_s = 0.011$ and $N_t/M = 0.56$, which was the last point for which the correlation of experimental data by eq 3 was possible.

the much larger region of surface coverages, up to 1.21 statistical monolayer coverage. The simpler form of this isotherm, in eq 4, not taking into account the effects of multilayer adsorption, made it possible to fit experimental data only in a limited region of submonolayer coverages smaller than 0.56 statistical coverage.

Let us mention that the function $Y(p)$ in eq 20 plotted now as a function of $-kT \ln X$ must be an increasing function at high p/p_s only in the region of applicability of the generalized fractal BET equation.

Now let us consider Figure 1, i.e., the nitrogen adsorption on the silica A200.

We can see here a similar region of p/p_s applicability of the simple eq 4 to that in Figure 1. However, as the solid line in Figure 1 is not a decreasing function at the highest p/p_s values it stimulates the question whether eq 4 and its extension, eq 19, are necessary to correlate experimental data. Moreover, it appears that using eq 4 makes even the agreement between theory and experiment worse. As β must be positive, all the attempts to fit by eq 4 the data at submonolayer coverages, decrease the number of the low-pressure points correlated by eq 4, i.e., lying below the inflection point now. This would suggest that in the region of the submonolayer coverages, eq 3 may be the exact equation in this case. In other words, the A200 surface seems to have a nature close to fully uncorrelated, i.e., ideally fractal surface. Such a situation would also suggest D values close to $D = 3$. Our numerical exercises fully supported these conclusions. After having performed many attempts to fit these experimental data, we discovered that the generalized BET fully fractal form of eq 3

$$Y = \ln \frac{N_t}{M\phi} = A_0 - A_1 kT \ln X - A_2 (kT)^2 [\ln X]^2 \quad (21)$$

leads to the best correlation of experimental data for nitrogen adsorption by the A200 silica, where A_0 , A_1 , and A_2 have the same meaning as in eq 19.

Figure 6 shows the best agreement between theory and experiment, at which we arrived while assuming that $D = 3$

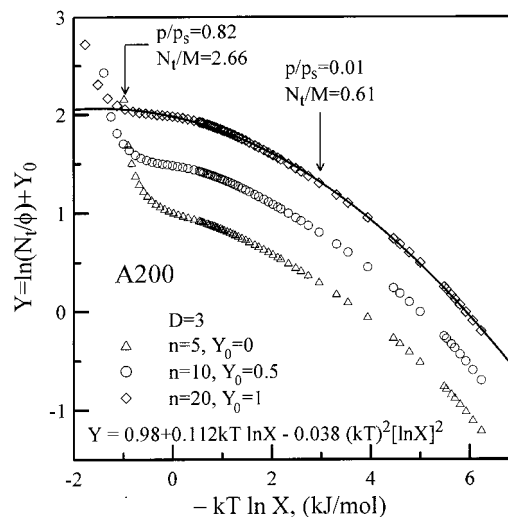


Figure 6. Application of eq 21 to correlate the experimental data for nitrogen adsorption by the A200 silica. The solid line (—) shows the best ever agreement which we obtained by assuming that $D = 3$ and $n = 20$. The coefficients A_0 , A_1 , and A_2 of the approximation by the quadratic function are also displayed. The arrow on the left-hand side indicates the range of the applicability (up to the inflection point on $Y(p/p_s)$) of eq 21, whereas the right-hand side arrow indicates the range of the applicability of eq 3 not taking into account the effects of multilayer adsorption.

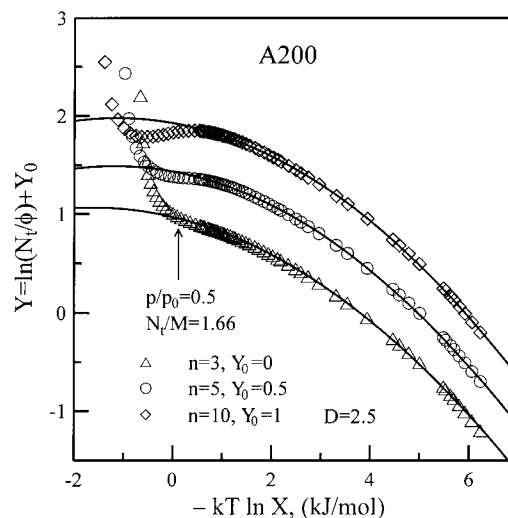


Figure 7. Attempts to correlate the data for nitrogen adsorption by the A200 silica, based on using eq 21 and assuming that $D = 2.5$. The arrow indicates the largest region of the applicability observed when assuming that $n = 3$.

and $n = 20$. The assumption that $D < 3$ led always to a worse agreement between theory and experiment. This is demonstrated in Figure 7.

Our finding is in excellent agreement with the estimation of the fractal dimensions of silica gels made by other methods and reported by Avnir et al.²³

5. Recovering the Adsorption Energy Distribution. Having estimated the parameters A_0 , A_1 , and A_2 , we can evaluate, by solving the equation system (eq 19a–c), the parameters α , β , and ϵ_0 of the adsorption energy distribution (eq 36), characterizing the energetic heterogeneity of the TN330 activated carbon. In the case of the A200 silica, in view of the applicability of eq 21, the corresponding energy distribution $\chi(\epsilon)$ is defined in eq 37. However, also in this case, the parameters α , β , and ϵ_0 are found by solving the equation system (19a–c). Table 1 collects the energetic parameters evaluated in that way.

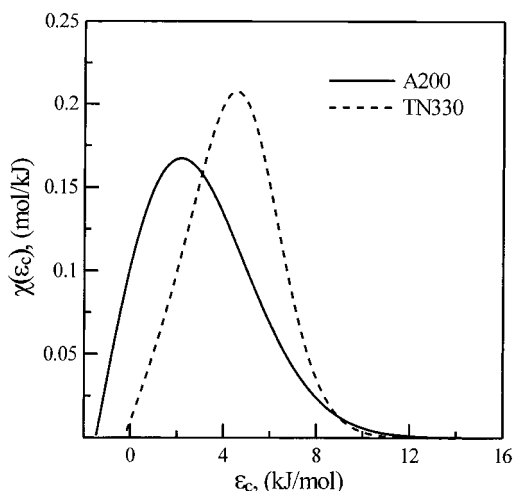


Figure 8. The adsorption energy distributions $\chi(\epsilon_c)$, calculated by using the parameters collected in Table 1. The solid line (—) is the $\chi(\epsilon_c)$ function calculated from eq 36 for nitrogen adsorption by the A200 silica, whereas the broken line (---) is the $\chi(\epsilon_c)$ function calculated from eq 36 for nitrogen adsorption by the activated carbon TN330.

TABLE 1: The Energetic Parameters Found by Solving the Equation System (Equation 19a–c)

adsorbent	α , kJ/mol	β , (kJ/mol) ²	ϵ_0 , kJ/mol	ϵ_1 , kJ/mol (from eq 23)	ϵ_1 , kJ/mol (inflection point)
TN330	0.505	0.069	3.41	−0.025	0.0
A200	0.199	0.038	1.145	−1.49	−1.0

The function $\chi(\epsilon_c)$ has physical meaning only in the domain of ϵ_c where $\chi(\epsilon_c)$ takes positive values, i.e., when

$$\alpha + 2\beta(\epsilon_c - \epsilon_0) \geq 0 \quad (22)$$

Therefore, the lowest value of ϵ_c , denoted later as ϵ_1 , is given by

$$\epsilon_1 = \frac{1}{2\beta}(2\beta\epsilon_0 - \alpha) = \frac{A_1}{2A_2} \quad (23)$$

Thus, while evaluating $\chi(\epsilon_c)$ defined either in eq 36 or in eq 37, these functions must be normalized to unity upon the limits $(\epsilon_1, +\infty)$, as shown in Figure 8. It is natural to assume that the value of $\epsilon_c = \epsilon_1$ corresponds to the highest adsorbate pressures at which our generalized fractal BET eqs 19 or 21 are applicable. The function $Y(p/p_s)$ takes then the highest physically meaningful value. Let us assume that indeed this is the highest value of Y which may be achieved in a real adsorption system. As the function $Y(p/p_s)$ describes approximately the surface coverage by the first adsorbed layer, that means, at $\epsilon_c < \epsilon_1$, the adsorption is likely to follow another mechanism forced by the condition $Y = \text{const}$. Indeed, Figures 5 and 6 show then an unusually rapid increase of adsorption, not predicted by our generalized fractal BET model.

Looking to Figure 5 we can see that $p/p_s = 0.48$ is the highest pressure at which our generalized fractal BET equation is applicable. Assuming, thus, that $\epsilon_c(p/p_s = 1/2) = \epsilon_1$, we arrive at the conclusion that $\epsilon_1 \approx 0$, in accordance with the value ϵ_1 estimated from eq 23. This would suggest that in the case of nitrogen adsorption by the activated carbon TN330 the choice $p'_0 = p_s$ is correct, because it leads to a consistent thermodynamic description.

In Figure 6, the highest value of p/p_s at which our generalized fractal BET equation is still applicable suggests $\epsilon_1 \approx 1$ kJ/mol.

This value is smaller than the value $\epsilon_1 \approx 1.5$ kJ/mol, found from eq 23. One possible explanation may involve the assumption that, in the case of nitrogen adsorbed on the A200 silica, the choice of $p'_0 = p_s$ is fairly good, but not an exact one.

This should not surprise one. Let us mention at this moment the somewhat forgotten papers published by Anderson²⁴ in 1946 and by Dole²⁵ in 1947. In their statistical thermodynamic considerations of multilayer adsorption, they emphasized the necessity of distinguishing in the BET model between the molecular partition function q in the second and higher layers, and the molecular partition function q_L in the bulk liquid state. Both these authors suggested that in the BET equation the value of X should be written as $\zeta p/p_s$, where $0 < \zeta < 1$. Thus, we decided to carry out an extensive numerical investigation to see, whether the choice $p'_0 > p_s$ could lead to a better agreement between the value of ϵ_1 found from eq 23, and estimated from the inflection point on the function $Y(p/p_s)$. It appeared, however, that no choice of p'_0 , D , or n could lead to a better result except that presented in Figure 6.

Another explanation may involve the assumption that this small discrepancy between the two ϵ_1 values may be due to neglecting interactions between the adsorbed molecules. Thus, we decided to take into consideration at least a part of these possible interactions between the molecules adsorbed in the first adsorbed layer. Because the function $N_t/(M\phi)$ is a fairly good estimation of the coverage in the first adsorbed layer, we repeated our calculations by adding to ϵ_c defined in eq 14 the interaction term defined in eq 1.73.²⁸ Thus, we used the following more general expression for ϵ_c :

$$\epsilon_c = -kT \ln X - \omega z \frac{N_t}{M\phi} \quad (24)$$

because that kind of generalization is correct for the system in which $D \approx 3$.

The highest possible value of z is 6 (hexagonal lattice), and the highest possible value of ω is 0.8 kJ/mol (the depth of the interaction potential between two nitrogen molecules). However, also the assumption that $\omega z > 0$ did not lead to a better agreement between these two ϵ_1 values than that presented in Figure 6. Therefore, the last possible explanation for the difference between these two ϵ_1 values in Table 1 might be the following.

The maximum value $n = 20$ found in our best-fit exercises for nitrogen adsorbed by the A200 silica means a large pore distribution of pore sizes ranging from about 0.40 to about 8 nm. It is, therefore, to be expected that n varies from low values up to 20 as the adsorption proceeds from small to larger and larger pores. Meanwhile, we used a constant value of n to arrive at the fit of experimental data presented in Figure 6. That constant value means an effective (maximum) value leading to that best fit but does not take into account the variation of n when the adsorption proceeds. This variation of n may not be so essential in the case of the activated carbon TN330 where the pore range is much narrower, but may play a certain role in the case of the A200 silica having much wider pore size distribution. Moreover, because $D \approx 3$, this is almost a constant distribution; therefore, no particular value of n is more probable than others.

This may suggest that in the case $D \rightarrow 3$ the distribution of n discussed by Cole et al.¹⁵ (eq 18) may play a certain role. However, it is to be expected that the fitting of an experimental isotherm will be sensitive to n basically at high surface coverages; therefore, choosing the constant n should lead to a reasonably good estimation of the maximum value of n .

6. Recovering the Geometric Surface Heterogeneities.

Since the early stage of the studies of adsorption on solids, the surface geometric heterogeneities have been believed to be a very important physical factor affecting the adsorption processes. Here the pore size distribution is the most commonly searched for characteristics of that geometric surface heterogeneity.

First successful attempts to recover the pore size distribution from the experimental isotherms were limited to adsorption in mesopores, where the capillary condensation can take place, and Kelvin equation may be applied for that purpose. The latest refinements of this method have been discussed by Kruk and Jaroniec.²⁶ Meanwhile, recovering the pore size distribution in the region of micropores, still remains a great challenge for adsorption scientists. Many papers have already been devoted to that problem, and almost all of them were based on solving the following integral equation:

$$\theta_i(p,T) = \int_{r_i}^{r_m} \left(\frac{\partial V}{\partial r} \right) \theta(r,p,T) dr \quad (25)$$

where $(\partial V/\partial r)$ is the searched pore size (volume) distribution, $\theta_i(p,T)$ is the experimentally measured isotherm, whereas the “local” isotherm $\theta(r,p,T)$ is calculated in a way using the methods of phenomenological and statistical thermodynamics, and computer simulations. (the density functional theory, and the non-local approximation, the smoothed density approximation, Monte Carlo, and molecular dynamics methods). It would be far beyond the scope of this paper to quote even the most relevant papers and reviews.

The method applied here belongs to the methods called “classical” by Lastoskie et al.³ It consists of assuming that the adsorption proceeds in a stepwise fashion in the sequence of decreasing (free) energies of adsorption ϵ_c , and that there exists a functional relationship between ϵ_c and r . Therefore, eq 25 can be rewritten as follows:

$$\theta_i(p,T) = - \int_{\epsilon_i}^{\epsilon_m} \left(\frac{\partial V}{\partial r} \right) \left(\frac{dr}{d\epsilon_c} \right) \theta_c d\epsilon_c \quad (26)$$

where θ_c is defined in eq I.4.²⁸ Then,

$$\frac{\partial V}{\partial r} \frac{dr}{d\epsilon_c} = \frac{\partial \theta_i}{\partial \epsilon_c} = -\chi_c(\epsilon_c) \quad (27)$$

Because the function $\chi_c(\epsilon_c)$ is calculated from experimental data, the main problem lies in calculating the function $(dr/d\epsilon_c)$. The works devoted to this problem have been reviewed recently by Jaroniec and Choma.²⁷

In our work, we postulate that there exists a general functional relationship $r(\epsilon_c)$, defined in eq I.23.²⁸ Accepting that postulate, and the related Taylor expansion I.24,²⁸ makes it possible to develop the generalized adsorption energy distributions I.36²⁸ and I.37²⁸ which explain the theoretical origin of all the empirical adsorption isotherms.

As we have shown, the function $r(\epsilon_c)$ can be obtained by fitting the experimental adsorption isotherm by corresponding to theoretical isotherms 19 and 21, for instance. Figure 9 shows this function for nitrogen adsorbed by the TN330 activated carbon.

The function $r(\epsilon_c)$ in Figure 9 was calculated up to the value $\epsilon_c = \epsilon_i$. It seems natural to assume that the related value of the dimensionless radius $r = 2.52$ corresponds to the maximum dimension of the pores in the TN330 activated carbon.

Next, it is natural to assume that the largest pores are those accommodating the $n = 4$ nitrogen molecules. This would

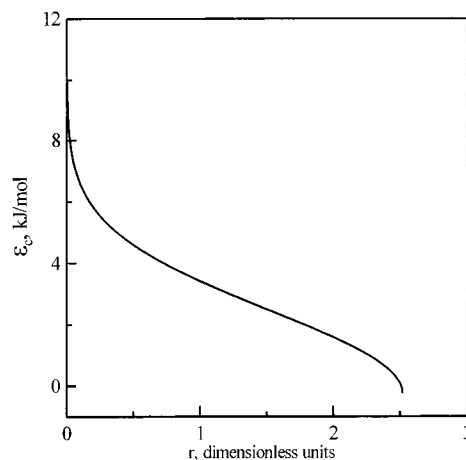


Figure 9. The $\epsilon_c(r)$ functions calculated for nitrogen adsorbed by the TN330 activated carbon, using the parameters collected in Table 1.

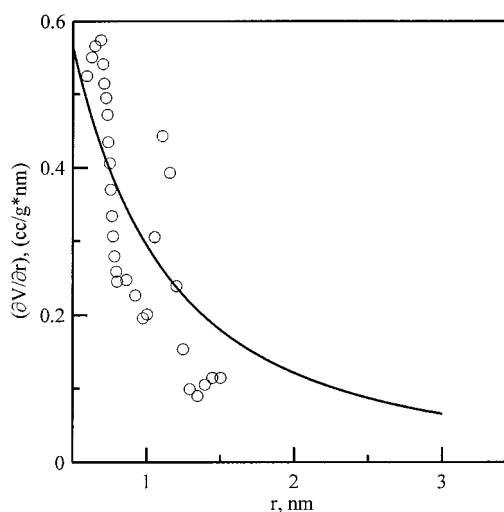


Figure 10. The comparison of the $(\partial V/\partial r)$ function, calculated by Jaroniec and Choma for the activated carbon BPL (○), with the $(\partial V/\partial r)$ function obtained here by us (—) for the TN330 activated carbon.

suggest that the maximum pore radius is about 2 nm, in accordance with the typical values reported in the literature.²⁷ We accept this estimation to draw the $(\partial V/\partial r)$ function characterizing the TN330 activated carbon. In Figure 10, this function is compared to the function $(\partial V/\partial r)$ calculated by Jaroniec and Choma²⁷ for the well-known BPL activated carbon. This comparison is only to show that the behavior of our $(\partial V/\partial r)$ function is typical of activated carbons. Thus, our initially calculated function $(\partial N/\partial r)$ was multiplied by a certain constant to arrive at $(\partial V/\partial r)$ values, comparable with those reported by Jaroniec and Choma²⁷ for the activated carbon BPL.

Jaroniec and Choma also used eq 27 to arrive at their $(\partial V/\partial r)$ function, but used the Horvath–Kawazoe method to calculate $(dr/d\epsilon_c)$. Let us mention that their $(\partial V/\partial r)$ function is similar to the $(\partial V/\partial r)$ functions calculated by Lastoskie et al.³ using eq 25 and the density functional theory to calculate $\theta(r,p,T)$.

As shown in Figure 10, our fractal $(\partial V/\partial r)$ function represents very typical geometric features of activated carbons.

The fractal pore size distribution is an universal function describing the fundamental features of all heterogeneous solid surfaces. As such, it loses certain individual features characteristic for a particular adsorption system under investigation. However, the attempts to arrive at more detailed characteristics

of an adsorption system may involve also a certain risk due to the lack of sufficient knowledge about the system.

Calculations of the function $\theta(p,p,t)$ are sensitive to the assumed shape of the pores. Next, the function $\theta(r,p,T)$ may not only be influenced by the r value but also by the presence of various functional groups. Such a situation is typical of activated carbons, for instance. Quite often, the calculations of the gas/solid potential function in pores of various geometries are accompanied by the assumption that pore walls are regular (homogeneous) structures. Thus, despite the impressive progress observed in the theories of adsorption by microporous materials, the fractal pore distribution estimated from the experimental adsorption isotherms may still represent valuable if not sufficient for many purposes information. Calculating that fractal pore size distribution does not involve any assumption about the detailed pore structure.

Summary

Most of the solids important for adsorption processes are heterogeneous. Their surface structure is a hybrid between a hypothetical perfectly organized, crystallographic-like structure, and a fully amorphous structure having no degree of organization. In the geometric terms that surface heterogeneity is considered as a collection of connected and disconnected pores having various radii. The commonly used quantitative characterization of that geometric surface heterogeneity is the pore size distribution function.

That geometric surface heterogeneity causes a variation in the gas–solid potential function on various areas of surface. This effect is called the energetic surface heterogeneity. The commonly used quantitative measure of this energetic heterogeneity is the differential distribution of the number of the local minima in the gas–solid potential function among the values of the adsorption potentials in these local minima. That function is commonly called the adsorption energy distribution. It can be recovered from the experimental adsorption isotherms by using various theoretical methods.

Despite a large variety of gas–solid systems which one may have to deal with, it appears that the experimental adsorption isotherms can be well described by only three simple empirical isotherms, i.e., Dubinin–Radushkevich, Freundlich, and Langmuir–Freundlich isotherms, starting from very low up to the monolayer surface coverages.

Next it was theoretically shown that there exists a certain function describing the surface energetic heterogeneity of all heterogeneous solid surfaces. Individual features of a gas–solid system are coded in the values of few (basically three) parameters appearing in that function.

By using the condensation approximation approach, one can show that the isotherm equation corresponding to that universal adsorption energy distribution predicts the applicability of DR isotherm at very low surface coverages, of the Freundlich isotherm at somewhat higher but still low surface coverages, and of the Langmuir–Freundlich isotherm at still higher submonolayer coverages. The analytical form of that general adsorption isotherm is a hybrid between these three simple isotherm equations. Application of that generalized isotherm equation to correlate the experimental adsorption isotherms shows that, indeed, their behavior is a hybrid between the features predicted by the DR, Freundlich, and Langmuir–Freundlich isotherms. By introducing corrections for the effects of multilayer adsorption, one arrives at an isotherm equation correlating experimental adsorption isotherms from very low, up to two statistical monolayer coverages.

The existence of the universal function describing the surface energetic heterogeneity of all solid surfaces, must suggest also existence of an universal pore distribution function which is the primary source of that energetic heterogeneity. The first successful attempts to find such a function were based on applying the concepts of the fractal geometry to characterize the surface geometric heterogeneity.

However, as the fractal geometry is basically applicable to fully amorphous structures, various deviations from the expected fractal behavior were reported. The reason for that seems to be obvious. The actual heterogeneous surfaces still exhibit a certain degree of surface organization, i.e., they are not fully amorphous. Also, that classical fractal approach resulted in a limited number of theoretically advanced papers reporting on new isotherm equations. The reason for that was the lack of a general expression that would create links between the geometric and energetic quantities. The latter are necessary to calculate the system partition function using the methods of statistical thermodynamics.

Looking to the reported theoretical calculations of the gas–solid interactions in pores, the general form of that interrelation $r = \exp\{-F(\epsilon)\}$ has been launched by us. Next, we have shown that to arrive from the pore distribution function, at that already known universal form of the adsorption energy distribution, a certain modification of the classical fractal pore size distribution is necessary. That modified pore size distribution reduces to the classical fractal distribution when $r \rightarrow 0$ and/or $D \rightarrow 3$, i.e., under the conditions where the classical fractal approach was, commonly, applicable. So, we have launched the hypothesis that this empirical correction takes into account the partial degree of organization of the actual heterogeneous solid surfaces.

To prove our hypothesis we used the modified fractal pore distribution to develop the general expression describing the effects of the interactions between the adsorbed molecules. We did it in the following way.

Assuming that the classical fractal pore size distribution describes the features of fully amorphous surfaces, and our modified pore size distribution is valid for partially organized (correlated) surfaces, we developed the corresponding two-pore distribution (correlation) function. That function and the mean-field-approximation were next used to develop the expression for the interaction term. The obtained expression considered as a function of the surface coverage θ_i was next compared to the two already known expressions: one describing the interactions on fully random, amorphous surfaces and the other one developed for perfectly organized (fully correlated) surfaces. The values of our newly developed expression lie between them, i.e., between the values predicted for fully amorphous and perfectly organized surfaces.

The second part of this publication was aimed at demonstrating the applicability of the modified fractal approach to correlate experimental data, and to analyze the physical meaning (thermodynamic consistency) of the results of our numerical analysis.

Two adsorption systems, representing two large classes of frequently investigated and applied in practice adsorption systems, were selected for that purpose. One of them was the popular, commercially available A200 silica, and another one was activated carbon, also commercially offered. We had at our disposal nitrogen adsorption isotherms, carefully measured starting from very low pressures, up to those close to the saturation pressure. This made a reliable theoretical/numerical analysis possible.

To extend our analysis to possibly largest range of surface coverages, we applied the BET adsorption model, modified by

Fripiat et al. to account for the fractality effects on the formation of the second and higher layers. Their fractal BET equation was next further generalized by us to take into account also the fractality energetic effects on the adsorption in the first layer closest to the surface. For that purpose, the generalized adsorption energy distribution was applied, developed from the modified fractal pore distribution, taking into account the partial degree of surface organization.

The Fripiat's BET equation generalized by us could be successfully used to correlate these two adsorption isotherms, in a large region of surface coverages up to 2.6 statistical monolayer coverage in the case of the A200 silica, and 1.2 statistical coverage in the case of the TN330 activated carbon. Beyond these coverages a very rapid multilayer adsorption started, which could not be described in terms of the BET model. This multilayer adsorption could not be also analyzed by using the "fractal FHH" equations. Therefore, we limited our analysis to the large pressure (coverage) range where our generalized fractal BET equation was applicable.

The results of our theoretical/numerical analysis provided us with a set of parameters creating a consistent thermodynamic and molecular picture of the two analyzed adsorption systems.

We believe that our method of analysis based on applying the generalized fractal BET equation may appear attractive for many researchers interested in deducing a few fundamental quantitative characteristics of the investigated adsorption systems from experimental isotherms.

Acknowledgment. One of the authors W. Rudzinski wishes to express his thanks to the National Research Council of Taiwan ROC for the grant making his extended visit to Prof. Lee Shyi-Long's laboratory at the National Chung-Cheng University possible.

References and Notes

(1) Rudzinski, W.; Everett, D. H. *Adsorption of Gases on Heterogeneous Surfaces*; Academic Press: London, 1992.

- (2) Jaroniec, M.; Madey, R. *Physical Adsorption on Heterogeneous Solids*; Elsevier: New York, 1988.
- (3) Lastoskie, C. M.; Quirke, N.; Gubbins, K. E. Structure of Porous Adsorbents: Analysis Using Density Functional Theory and Molecular Simulation. In *Equilibria and Dynamics of Gas Adsorption on Heterogeneous Solid Surfaces*; Rudzinski, W., Steele, W. A., Zgrablich, G., Eds.; Elsevier: New York, 1997.
- (4) Ehrburger-Dolle, F. *Langmuir* **1997**, *13*, 1189.
- (5) Ehrburger-Dolle, F. *Langmuir* **1999**, *15*, 6004.
- (6) Cortes, J.; Araya, P. *J. Colloid Interface Sci.* **1987**, *115*, 271.
- (7) Pfeifer, P.; Kenntner, J.; Cole, M. W. *Proceedings of the Conference on Fundamentals of Adsorption*; Sonthofen, 1989.
- (8) Pfeifer, P.; Wu, J. Y.; Cole, M. W.; Krim, J. *J. Phys. Rev. Lett.* **1989**, *62*, 1877.
- (9) Avnir, D.; Jaroniec, M. *Langmuir* **1989**, *5*, 1431.
- (10) Cheng, E.; Cole, M. W.; Pfeifer, P. *Phys. Rev. B* **1989**, *39*, 12962.
- (11) Jaroniec, M.; Lu, X.; Madey, R.; Avnir, D. *J. Chem. Phys.* **1990**, *92*, 7589.
- (12) Pfeifer, P.; Cole, M. W. *New J. Chem.* **1990**, *14*, 221.
- (13) Yin, Y. *Langmuir* **1991**, *7*, 216.
- (14) Waksmundzki, A.; Rudzinski, W.; Sokolowski, S.; Jaroniec, M. *Pol. J. Chem.* **1974**, *48*, 1741.
- (15) Cole, M. W.; Holter, N. S.; Pfeifer, P. *Phys. Rev. B* **1986**, *33*, 8806.
- (16) Levitz, P.; Van Damme, H.; Fripiat, J. *Langmuir* **1988**, *4*, 781.
- (17) Hill, T. L. *Statistical Mechanics*; McGraw-Hill: New York, 1956.
- (18) Wojsz, R.; Terzyk, A. P. *Comput. Chem.* **1996**, *20*, 427.
- (19) Terzyk, A. P.; Wojsz, R.; Rychlicki, G.; Gauden, P. *Colloids Surf.* **1996**, *119*, 175.
- (20) Terzyk, A. P.; Wojsz, R.; Rychlicki, G.; Gauden, P. *Colloids Surf.* **1997**, *126*, 67.
- (21) Terzyk, A. P.; Gauden, P.; Rychlicki, G.; Wojsz, R. *Colloids Surf.* **1998**, *136*, 245.
- (22) Terzyk, A. P.; Gauden, P.; Rychlicki, G.; Wojsz, R. *Colloids Surf.* **1999**, *152*, 293.
- (23) Avnir, D.; Farin, D.; Pfeifer, P. *J. Colloid Interface Sci.* **1985**, *103*, 112.
- (24) Anderson, R. B. *J. Am. Chem. Soc.* **1946**, *68*, 686.
- (25) Dole, M. *J. Chem. Phys.* **1948**, *16*, 25.
- (26) Kruk, M.; Jaroniec, M. *Langmuir* **1997**, *13*, 6267.
- (27) Jaroniec, M.; Choma, J. Characterization of Geometrical and Energetic Heterogeneities of Active Carbons by Using Sorption Measurements. In *Equilibria and Dynamics of Gas Adsorption on Heterogeneous Solid Surfaces*; Rudzinski, W., Steele, W. A., Zgrablich, G., Eds.; Elsevier: New York, 1997.
- (28) Rudzinski, W.; Shyi-Long, L.; Panczyk, T.; Ching-Cher Sanders, Y. *J. Phys. Chem. B* **2001**, *105*, 10847.